

Density Functional Theory Study of Gas Phase Hydrolysis of Titanium Tetrachloride[#]

Ani K. John,[2] S. Savithri,[1] Kunduchi P. Vijayalakshmi,[1] and Cherumuttathu H. Suresh*[1]

[1]Computational Modeling and Simulation Section, National Institute for Interdisciplinary Science and Technology (CSIR), Trivandrum 695-019, India

[2]Project Engineering and Productionization Facilities, Vikram Sarabhai Space Centre, ISRO, Trivandrum 695-022, India

Received January 5, 2010; E-mail: sureshch@gmail.com

Thermodynamic parameters of four elementary steps of hydrolysis of $TiCl_4$, viz. formation of (i) $TiCl_3(OH)$, (ii) $TiCl_2(OH)_2$, (iii) $TiCl(OH)_3$, and (iv) $Ti(OH)_4$ as well as condensation of the hydroxides giving rise to titanoxanes ($Cl_{4-x}(OH)_{x-1}Ti–O–TiCl_{4-x}(OH)_{x-1}$ ($x = 1$–4)) have been studied using B3LYP/6-311++G(d,p) level of DFT. The first elementary step required the highest free energy of activation ($\Delta G^{\#} = 22.8$ kcal mol^{-1}) as well as the highest enthalpy of activation ($\Delta H^{\#} = 16.9$ kcal mol^{-1}), while subsequent steps showed a decrease in both $\Delta G^{\#}$ and $\Delta H^{\#}$, reaching the lowest value of $\Delta G^{\#} = 20.4$ kcal mol^{-1} and $\Delta H^{\#} = 11.9$ kcal mol^{-1} for the fourth step. Condensation reactions were triggered by O–H···O–H hydrogen bonding in pre-reactant complexes. The $\Delta G^{\#}$ of the condensation of mono-, di-, tri-, and tetrahydroxides are 23.0, 17.1, 20.8, and 14.5 kcal mol^{-1}, respectively. Thus gas phase hydrolysis of $TiCl_4$ and subsequent condensation of $TiCl_{4-x}(OH)_x$ are feasible at low temperature and higher order condensation would lead to the formation of TiO_2. $TiCl_4$ showed higher Lewis acid character to a water dimer than a water molecule as their respetive interaction energies were -4.8 and -14.2 kcal mol^{-1}. Coordination of the water dimer to titanium has significant effect on lowering the activation bariers of the hydrolysis reactions and therefore the amount of water vapor in the gas phase reaction is critical to the overall rate of the reaction.

Titanium dioxide (TiO_2) commonly known as titania is one of the most extensively studied materials, both experimentally and theoretically due to its particular physical and chemical properties such as high refractive index, excellent optical transmittance in the visible and near-infrared regions, high dielectric constant,[1,2] and UV-induced electron excitation.[3] Nanosized titania has a high surface area to volume ratio making it useful as a photocatalyst,[3,4] in solar cells for the production of hydrogen and electric energy, as a gas sensor, as white pigment, as colored ceramic pigment, as a corrosion-protective coating, as an optical coating, and in electronic and electrical devices.[5] One of the cheap precursors for the synthesis of titania nanoparticles is titanium tetrachloride ($TiCl_4$). Oxidation of $TiCl_4$ is carried out at as high as 1400 °C, making more than half of the annual world wide consumption of over 3 million tons of TiO_2.[6,7] But this high temperature method has some serious draw backs such as difficulty in controlling product characteristics, corrosion of reactor, suitability of material of construction, formation of corrosive gases, and operational problems from high temperatures. In earlier work,[8,9] we have clearly pointed out that the low temperature vapor phase hydrolysis of $TiCl_4$ to produce TiO_2 offers several advantages such as product purity, ease of collection, energy efficiency and absence of unit operations of filtration, washing and drying involving large liquid volumes, etc. Thus gas phase low temperature studies on the mechanism of $TiCl_4$ hydrolysis and condensation of hydrolyzed products become of fundamental importance as they would provide deeper insight to particle clustering chemistry and particle nucleation. However, experimental measurements of the thermochemical properties are usually expensive and difficult for a metal-mediated fast reaction and in addition, the sheer number of relevant chemical species involved in various stages of the reaction can hinder the construction of an appropriate experimental database. Therefore, it is highly desirable to use computational chemistry techniques as alternatives to analyze various steps of complicated reactions. Recent developments of quantum chemical ab initio and density functional theory (DFT) methods and fast progress in computational hardware have provided theoretical quantum chemistry approaches as an alternative to even experiments. In this paper we have considered initial reactions between $TiCl_4$ and H_2O as well as condensation titanium hydroxides to provide some insight into the thermochemistry, mechanism and kinetics of vapor phase hydrolysis of $TiCl_4$ in an aerosol reactor.

Computational Details

For most of the calculations including the geometry optimization and also for the calculation of reaction paths, the widely used B3LYP DFT method was used.[10,11] The B3LYP method has been reported to provide excellent descriptions of various reaction profiles and particularly of geometries, heats of reaction, activation energies, and vibrational properties of various molecules.[12–15] To reduce the basis set superposition error (BSSE) to a negligible level in energy calculations, the triple zeta level 6-311++G(d,p) basis set was chosen. However, in order to assess the reliability of the method, selected systems have been also optimized using the

Published on the web September 2, 2010; doi:10.1246/bcsj.20100001

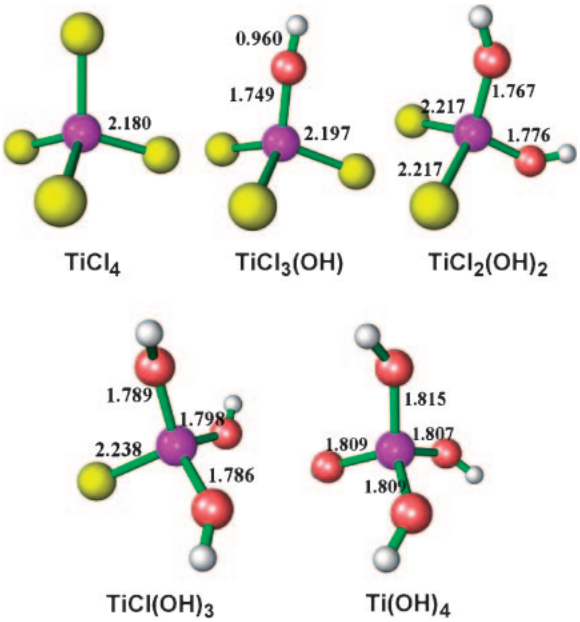

Figure 1. B3LYP/6-311++G(d,p) level optimized geometries of four coordinated titanium compounds: $TiCl_4$, $TiCl_3(OH)$, $TiCl_2(OH)_2$, $TiCl(OH)_3$, and $Ti(OH)_4$. Distances in Å.

recently developed DFT method of MPWB1K[16–18] and the ab initio second order Möller–Plesset perturbation theory (MP2)[19,20] method. All DFT functionals were used as implemented in the Gaussian03 program package.[21] Thermal contributions to the energetic properties were also calculated at 298.15 K and 1 atm. The enthalpy (H) and Gibbs free energy (G) values computed using B3LYP/6-311++G(d,p) method is used for constructing the respective energy profiles depicted in all the figures. The intrinsic reaction coordinate (IRC) was traced to verify the connectivity of the reactants and products to the transition state by solving the IRC equation with an algorithm developed by Gonzalez and Schlegel[22] as implemented in Gaussian03.

Results and Discussion

Tetrahedral $TiCl_{4-x}(OH)_x$ ($x = 0$–4) Systems. The optimized geometries and bond length parameters of $TiCl_4$, $TiCl_3(OH)$, $TiCl_2(OH)_2$, $TiCl(OH)_3$, and $Ti(OH)_4$ at B3LYP/6-311++G(d,p) level are presented in Figure 1. Consecutive substitution of Cl by OH in the $TiCl_{4-x}(OH)_x$ ($x = 0$–4) series leads to elongation of both Ti–Cl and Ti–O bond lengths. Thus the first two molecules in the series, $TiCl_4$ and $TiCl_3(OH)$, have the shortest Ti–Cl (2.180 Å) and Ti–O (1.749 Å) bonds, respectively, while the last two in the series, $TiCl(OH)_3$ and $Ti(OH)_4$ have the longest Ti–Cl (2.238 Å) and Ti–O (1.815 Å) bonds, respectively.

Experimental structures and vibrational frequencies are available only for $TiCl_4$[23] and $Ti(OH)_4$.[24] In Table 1, the computed vibrational frequencies of $TiCl_4$ are compared along with the experimental and previous theoretical results. The present results agree better with experimental values[25] than earlier theoretical studies using HF ECP (effective core potential),[26] B3LYP,[27] and MP2[27] approaches. The experimental values for Ti–O stretch (766 cm^{-1}) and O–H stretch (3713 cm^{-1}) in $Ti(OH)_4$ also agree well with the respective computed values (average values of the four Ti–O and O–H stretches are 747 and 3913 cm^{-1}, respectively).[24] On the basis of these results, it is felt that the B3LYP/6-311++G(d,p) method is a good choice for the present study and this method is used throughout.

Table 1. Computed and Experimental Vibrational Frequencies (in cm^{-1}) for $TiCl_4$

Mode	B3LYP/ 6-311++G(d,p)	Exp.[25]	Calcd[26]	Calcd[27]	Calcd[27]
$\nu_1(e)$	115	118	96	121	122
$\nu_2(t_2)$	136	139	129	144	141
$\nu_3(a_1)$	383	388	377	397	407
$\nu_4(t_2)$	494	497	507	514	533

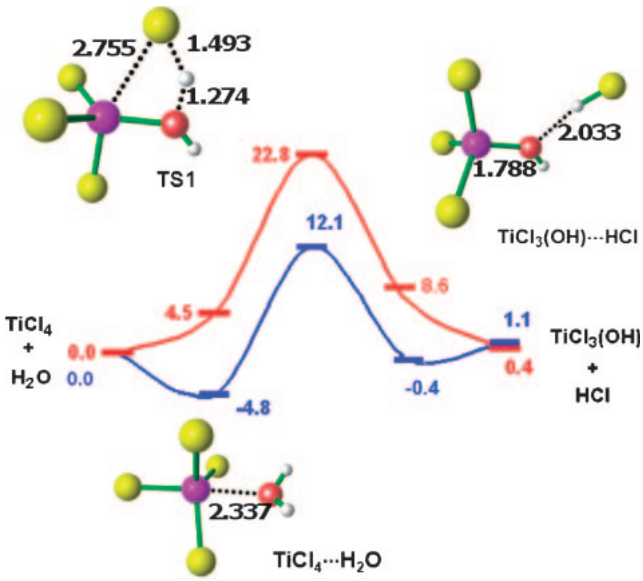

Figure 2. Relative enthalpy (blue) and relative free energy (pink) profiles for the elementary reaction (1). Distances in Å and energy in kcal mol^{-1}.

Elementary Reactions of $TiCl_4$ Hydrolysis. The commonly accepted mechanism for the hydrolysis of $TiCl_4$ can be represented by the four elementary reactions given below.

$$TiCl_4 + H_2O \rightarrow TiCl_3(OH) + HCl \quad (1)$$

$$TiCl_3(OH) + H_2O \rightarrow TiCl_2(OH)_2 + HCl \quad (2)$$

$$TiCl_2(OH)_2 + H_2O \rightarrow TiCl(OH)_3 + HCl \quad (3)$$

$$TiCl(OH)_3 + H_2O \rightarrow Ti(OH)_4 + HCl \quad (4)$$

The relative enthalpy (ΔH) and relative Gibbs free energy (ΔG) profiles are calculated for all these reactions using the B3LYP/6-311++G(d,p) method. In Figure 2, ΔH and ΔG profiles of reaction (1) are given along with the structures of five stationary points. In $TiCl_4$, the nucleophillic attack of H_2O is observed along the C_3 axis to yield a distorted triagonal bipyramidal $TiCl_4{\cdots}H_2O$ complex where the Ti–O distance is 2.337 Å. The formation of $TiCl_4{\cdots}H_2O$ is exothermic by

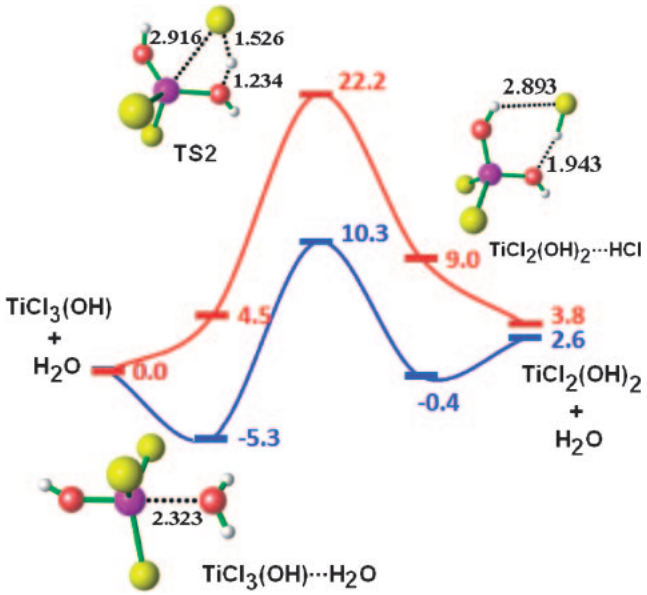

Figure 3. Enthalpy and free energy profiles for the elementary reaction (2). Distances in Å and energy values in kcal mol^{-1}.

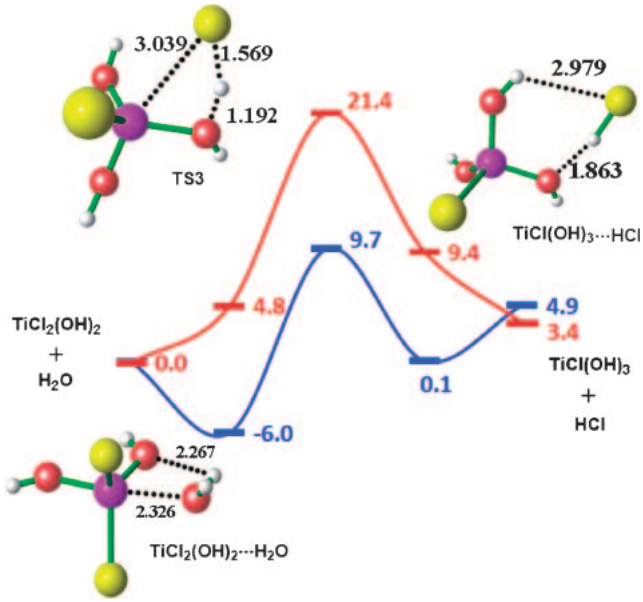

Figure 4. Enthalpy and free energy profiles for the elementary reaction (3). Distances in Å and energy values in kcal mol^{-1}.

4.8 kcal mol^{-1} (1 kcal mol^{-1} = 4.184 kJ mol^{-1}) and endergonic by 4.5 kcal mol^{-1}. The endergonic character is due to the loss of entropy as the coordination of H_2O to the metal leads to a decrease in the $T\Delta S$ term by 9.3 kcal mol^{-1} when compared to that of ($TiCl_4 + H_2O$). A four-center transition state TS1 simultaneously activates the O–H and Ti–Cl bonds to give $TiCl_3(OH)\cdots HCl$ complex. In TS1, partly broken O–H (1.274 Å), Ti–Cl (2.755 Å), and partly formed H–Cl (1.493 Å) bonds are present. The enthalpy of activation ($\Delta H^{\#}$) and free energy of activation ($\Delta G^{\#}$) are 16.9 and 22.8 kcal mol^{-1}, respectively. It may be noted that the $\Delta G^{\#}$ is calculated with respect to the ($TiCl_4 + H_2O$) and the transition state while the $\Delta H^{\#}$ is calculated with respect to $TiCl_4\cdots H_2O$ and the transition state. Throughout this paper we have used the free energy of the separated systems to quantify the $\Delta G^{\#}$ whereas the enthalpy of the associated systems for the calculation of the $\Delta H^{\#}$. The monohydroxide $TiCl_3(OH)$ will be formed when HCl is dissociated from the $TiCl_3(OH)\cdots HCl$ complex. Overall the reaction is endothermic by 1.1 kcal mol^{-1} and endergonic by 0.4 kcal mol^{-1}.

The ΔH and ΔG of reaction (2) (Figure 3) follow nearly the same trend as that of reaction (1). The coordination of H_2O to $TiCl_3(OH)$ occurs at a position trans to the OH group and the distance of the new Ti–O interaction is 0.014 Å shorter than the corresponding value in $TiCl_4\cdots H_2O$ indicating that the affinity of $TiCl_3(OH)$ for water coordination is higher than $TiCl_4$. This feature is also supported by the fact that $TiCl_4\cdots H_2O$ binding energy of 4.8 kcal mol^{-1} is 0.5 kcal mol^{-1} smaller than that of the $TiCl_3(OH)\cdots H_2O$ (Figures 2 and 3). The four-center transition state TS2 activates both Ti–Cl (2.916 Å) and the O–H (1.234 Å) bonds to yield HCl and $TiCl_2(OH)_2$. This process has to overcome a $\Delta G^{\#}$ of 22.2 kcal mol^{-1} ($\Delta H^{\#}$ is 15.6 kcal mol^{-1}) to reach the product system. The weakly bonded $TiCl_2(OH)_2\cdots HCl$ system may dissociate to the constituting molecules. Overall, the $TiCl_3(OH)$ hydrolysis appeared to be endothermic by 2.6 kcal mol^{-1} and endergonic by 3.8 kcal mol^{-1}.

In the third elementary reaction (Figure 4), the enthalpy is decreased by 6.0 kcal mol^{-1} when $TiCl_2(OH)_2\cdots H_2O$ complex is formed which is higher than the corresponding value for the formation of $TiCl_3(OH)\cdots H_2O$. However, the distance of interaction between H_2O and Ti atom in $TiCl_2(OH)_2\cdots H_2O$ (2.326 Å) is slightly higher than the value of 2.323 Å in $TiCl_3(OH)\cdots H_2O$. Therefore, the higher affinity of water to titanium dihydroxide is attributed to the presence of intramolecular $OH\cdots OH_2$ hydrogen bond. The H_2O has to overcome a $\Delta H^{\#}$ barrier of 15.7 kcal mol^{-1} ($\Delta G^{\#} = 21.4$ kcal mol^{-1}) in TS3 to reach $TiCl(OH)_3\cdots HCl$. The reaction is endothermic by 4.9 kcal mol^{-1} while the free energy is increased by 3.4 kcal mol^{-1}.

The ΔH and ΔG profiles for the elementary reaction (4) is shown in Figure 5. The energetics of the coordination of water molecule to $TiCl(OH)_3$ showed similar tendency to those observed in the previous elementary reactions. Although the TS4 appears to be similar to other transitions states, the Ti–Cl bond in this system showed the highest distance of 3.239 Å. In fact, along the TS1, TS2, TS3, and TS4 systems, Ti–Cl distance showed gradual elongation starting from the minimum of 2.755 Å in TS1 to the maximum of 3.239 Å in TS4. Compared to the elementary steps (1), (2), and (3), a noticeable change in reaction (4) is the decrease in the activation energy values ($\Delta H^{\#} = 11.9$ kcal mol^{-1} and $\Delta G^{\#} = 20.4$ kcal mol^{-1}). Overall, the formation of $Ti(OH)_4$ is found to be endothermic by 6.9 kcal mol^{-1} and endergonic by 9.6 kcal mol^{-1}.

It may be noted that the binding energy of water and $TiCl_{4-x}(OH)_x$ is -4.8, -5.3, -6.0, and -5.7 kcal mol^{-1} for $x = 0$, 1, 2, and 3, respectively suggesting that the metal center has a high affinity toward water coordination. On the other hand, the dissociation energy of $TiCl_{4-x}(OH)_x\cdots HCl$ complex is 0.8, 3.0, and 3.3 kcal mol^{-1} for $x = 1$, 2, and 3, respectively.

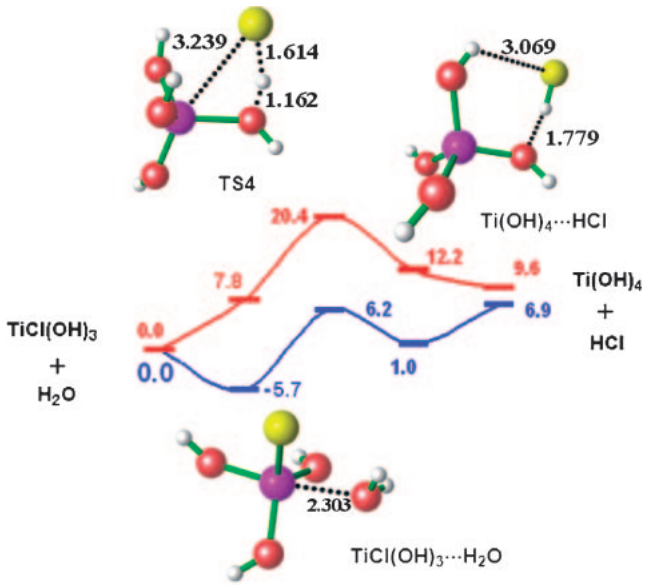

Figure 5. Enthalpy and free energy profiles for the elementary reaction (4). Distances in Å and energy values in kcal mol^{-1}.

Therefore, when the HCl bound product is formed, the HCl can be replaced with water molecule and as a consequence, the forward reactions will be enhanced in every step leading to facile hydrolysis of $TiCl_4$.

Dimerization Leading to Condensation of Titanium Hydroxides. Dimerization of titanium hydroxides would lead to condensation products with Ti–O–Ti bond connectivity. In all the four cases studied herein, viz. (a) monohydroxide, (b) dihydroxide, (c) trihydroxide, and (d) tetrahydroxide, the first step is the formation of hydrogen-bonded dimers through the interaction of the hydroxy groups. The energetics of the dimerization and the subsequent condensation step of the four cases (a, b, c, and d) are depicted in Figure 6. The enthalpy change associated with initial dimerization is found to be −3.6, −7.2, −7.2, and −10.0 kcal mol^{-1} for (a), (b), (c), and (d), respectively, which indicates that the tendency for dimerization in the higher hydroxides is quite high due to the increase in the number of OH···OH hydrogen bonds. Four-center transition states TS5, TS6, TS7, and TS8 are observed for the condensation steps of (a), (b), (c), and (d), respectively. These reactions can be classified as O–H bond metathesis as the oxidation state of the metal centers is unchanged during the process leading to the migration of a proton from one OH

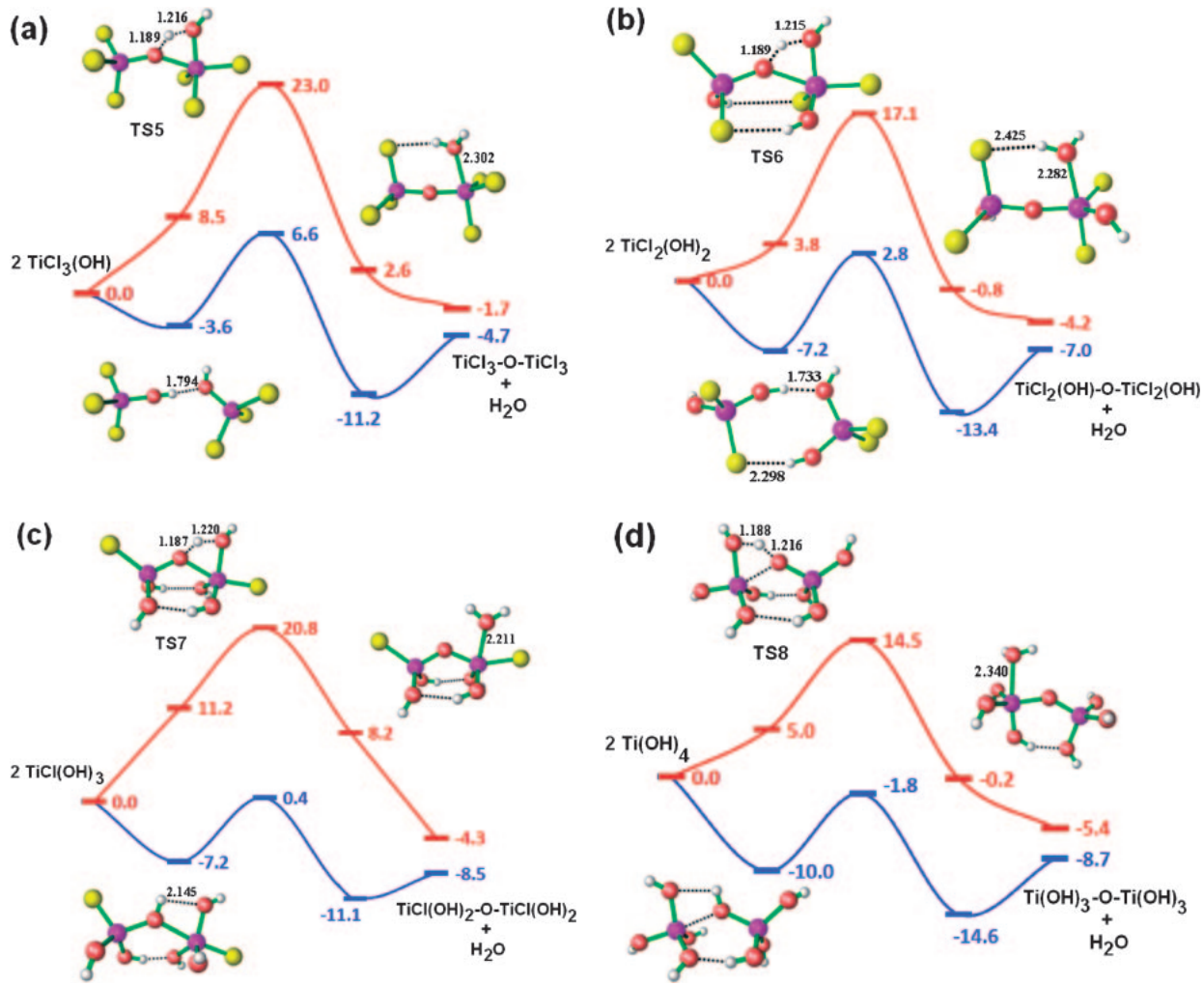

Figure 6. Enthalpy and free energy surfaces for the condensation reaction of $TiCl_{4-x}(OH)_x$; $x = 1$–4. Distances in Å and energy values in kcal mol^{-1}.

Table 2. Comparison of the Energy Effects of Elementary Hydrolysis Reaction for Titanium and Silicon Chlorides[a)]

Reaction	ΔH /kcal mol^{-1}	ΔG /kcal mol^{-1}	$\Delta H^{\#}$ /kcal mol^{-1}	$\Delta G^{\#}$ /kcal mol^{-1}
$TiCl_4 + H_2O \rightarrow TiCl_3(OH) + HCl$	1.1	0.4	16.9	22.8
$SiCl_4 + H_2O \rightarrow SiCl_3(OH) + HCl$	−5.6	−7.1	24.2	34.1
$TiCl_3(OH) + H_2O \rightarrow TiCl_2(OH)_2 + HCl$	2.6	3.8	15.6	22.2
$SiCl_3(OH) + H_2O \rightarrow SiCl_2(OH)_2 + HCl$	−5.6	−5.1	18.8	31.0
$TiCl_2(OH)_2 + H_2O \rightarrow TiCl(OH)_3 + HCl$	4.9	3.4	15.7	21.4
$SiCl_2(OH)_2 + H_2O \rightarrow SiCl(OH)_3 + HCl$	−5.0	−4.5	18.6	30.5
$TiCl(OH)_3 + H_2O \rightarrow Ti(OH)_4 + HCl$	6.9	9.6	11.9	20.4
$SiCl(OH)_3 + H_2O \rightarrow Si(OH)_4 + HCl$	−4.6	−3.7	15.2	27.6

a) The values for silicon systems are taken from Ref. 28.

group to another OH group. The resulting system is the water bound condensation product (Figure 6) which would further dissociate in to water and a condensation product characterized by a Ti–O–Ti bond connectivity. The values of $\Delta H^{\#}$ for the condensation step of (a), (b), (c), and (d) are 10.2, 10.0, 7.6, and 8.2 kcal mol^{-1}, respectively while the corresponding $\Delta G^{\#}$ values are 23.0, 17.1, 20.8, and 14.5 kcal mol^{-1}, respectively. It is obvious that the increase in number of hydroxide group around the metal center reduces the enthalpy of activation for the condensation. In fact, the formation of a more stable dimerization product also led to a more stable transition state, which means that the rate of condensation is expected to increase when the number of hydroxide group in the system is increased. In the case of elementary reactions, the lowest $\Delta H^{\#}$ and lowest $\Delta G^{\#}$ values are 12.2 and 20.4 kcal mol^{-1}, respectively (Figure 5) while in the case of condensation reactions, the highest $\Delta H^{\#}$ and highest $\Delta G^{\#}$ values are 10.2 and 23.0 kcal mol^{-1} (Figure 6), respectively. This indicates that the step-wise hydrolysis of $TiCl_4$ and the condensation reactions of the hydroxides are facile processes.

Comparison of the $TiCl_4$ and $SiCl_4$ Hydrolysis. Recently, $SiCl_4$ gas phase hydrolysis as well as the dimerization of $SiCl_{4-x}(OH)_x$ where $x = 0$–4 has been theoretically modeled by Ignatov et al.[28] using the B3LYP/6-311++G(2d,2p) level of DFT. The transition state models of these reactions showed a very close resemblance to the corresponding titanium analogs presented in this work. In Table 2, reactions involving $TiCl_4$ and $SiCl_4$ precursors are compared on the basis of their calculated enthalpy and Gibbs free energy changes (ΔH and ΔG) as well as the $\Delta H^{\#}$ and $\Delta G^{\#}$ values. In the case of elementary reactions, both the ΔH and ΔG values are higher for the titanium systems than the silicon systems whereas in the case of condensation reactions this energy ordering is reversed. For instance, the ΔG value of elementary reaction (4) is 9.6 kcal mol^{-1} for titanium and −3.7 kcal mol^{-1} for silicon. Though the silicon hydroxides are more stabilized than titanium hydroxides, the $\Delta H^{\#}$ and $\Delta G^{\#}$ values for the elementary reactions are lower in the case of titanium systems than silicon systems. For instance, the initial hydrolysis of $SiCl_4$ may not occur at room temperature considering the high $\Delta G^{\#}$ of 34.1 kcal mol^{-1} while such a reaction for $TiCl_4$ is expected to be facile at room temperature due to the smaller $\Delta G^{\#}$ of 22.8 kcal mol^{-1}. The energetics thus suggests facile hydrolysis of $TiCl_4$ at room temperature followed by rapid condensation of the titanium hydroxides. These results indicate

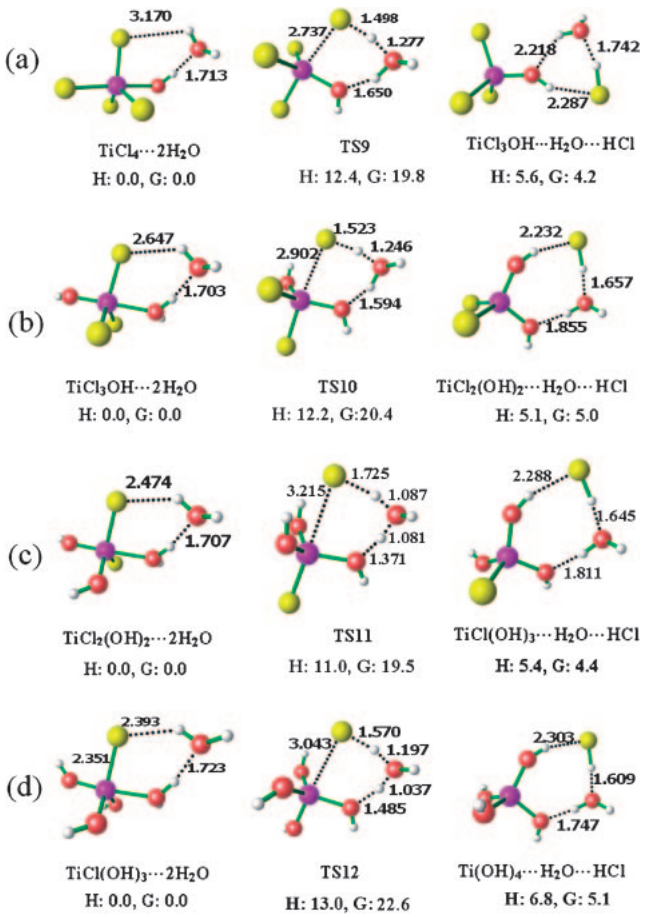

Figure 7. Mechanism of hydrolysis using two water molecules. Reactions corresponds to (a) $TiCl_4$, (b) $TiCl_3(OH)$, (c) $TiCl_2(OH)_2$, and (d) $TiCl(OH)_3$. Distances in Å and energy values in kcal mol^{-1}.

that the dimerization of $TiCl_{4-x}(OH)_x$ and the subsequent polymerization steps leading to TiO_2 formation could be a very fast and clean process even at room temperature. On the other hand, in the case of silicon systems, similar reactions may occur at elevated temperature and the possibility of the formation of unreacted hydroxides may be high.

Role of a Second Water Molecule in Hydrolysis Reaction. In this section, the role of a second water molecule in the mechanism of hydrolysis of $TiCl_4$ is described. The structures of $TiCl_{4-x}(OH)_x \cdot 2H_2O$ systems are depicted in Figure 7.

Table 3. Complex Formation Energies (in kcal mol^{-1}) for $TiCl_{4-x}(OH)_x \cdot yH_2O$ ($x = 0$–3, $y = 1$–2) Complexes

$TiCl_{4-x}(OH)_x \cdot yH_2O$	x:y	Enthalpy	Free energy
$TiCl_4$	1:1	−4.8	4.5
	1:2	−14.2	4.2
$TiCl_3(OH)$	1:1	−5.3	4.5
	1:2	−14.8	5.2
$TiCl_2(OH)_2$	1:1	−6.0	4.8
	1:2	−14.8	5.9
$TiCl(OH)_3$	1:1	−5.7	7.8
	1:2	−14.8	8.3

In Table 3, the energy released in the complexation of $TiCl_{4-x}(OH)_x$ ($x = 0$–3) with monomer H_2O and dimer H_2O are compared. The data clearly suggest that H_2O dimer has higher affinity to bind with $TiCl_{4-x}(OH)_x$ than H_2O. In $TiCl_{4-x}(OH)_x \cdot 2H_2O$, the oxygen coordination of the H_2O to the Ti center activates one of its O–H bonds: the one showing hydrogen-bond interaction with the second H_2O. This bond is easily cleaved when the $TiCl_{4-x}(OH)_x \cdot 2H_2O$ systems pass through the transition states TS9, TS10, TS11, and TS12, respectively for $x = 0$, 1, 2, and 3 (Figure 7).

The energetics in Figure 7 strongly suggest that more than one water molecule may participate in the elementary hydrolysis reactions. It may be noted that the ordered pairs of ($\Delta H^{\#}$, $\Delta G^{\#}$) in kcal mol^{-1} are (16.9, 22.8), (15.6, 22.2), (15.8, 21.4), and (11.9, 20.4), respectively for the elementary reactions (1), (2), (3), and (4) using one water molecule while the corresponding values of the reaction with water dimer are (12.4, 19.8), (12.2, 20.4), (11.0, 19.5), and (13.0, 22.6). The energetics suggest that the water dimer-assisted hydrolysis of the first three elementary reactions are more favorable than the reaction with single water molecule whereas the forth elementary reaction is more favorable in the presence of one water molecule.

Conclusion

A systematic study has been carried out to understand the elementary steps of the gas phase hydrolysis of $TiCl_4$ and subsequent condensation reactions of the hydroxide complexes using B3LYP/6-311++G(d,p) level of DFT method. The dimerization steps in the hydrolysis of titanium hydroxide systems have lower activation barriers than the primary hydrolysis of $TiCl_4$. Further, the condensation reactions lead to lowering of both enthalpy and free energy of the system. These results imply that the dimerization reaction should occur rapidly once initial monomer hydroxides are formed. This agrees with the experimental observation also,[29–32] the reactions prevail under conditions where water is in excess. Water has a high coordination power to the titanium center, and this affinity is enhanced with increase in the hydroxide moieties around the metal center which also suggests that the amount of water in the reaction medium is critical to the overall rate of the reaction. The interaction of a water dimer to the metal center has a profound effect on decreasing the activation barriers of the first three elementary processes. The thermodynamic data presented herein could be used as an input for modeling the formation of titania nanopowders through aerosol hydrolysis. Further research in this direction is underway.

The first author acknowledges the Department of Science and Technology, Govt. of India for the fellowship support. This article is dedicated to the memory of Dr. G. D. Surender, whose unfailing enthusiasm for research has been an inspiration to us. The optimized geometries and thermodynamic parameters of all the structures discussed in the text may be obtained on request from the authors.

Supporting Information

Optimized geometries and thermodynamic parameters of all the structures described in the paper. This material is available free of charge on the web at http://www.csj.jp/journals/bcsj/.

References

Dedicated to the memory of Dr. G. D. Surender.

1 H.-S. Kim, D. C. Gilmer, S. A. Campbell, D. L. Polla, *Appl. Phys. Lett.* **1996**, *69*, 3860.

2 X. Chen, S. S. Mao, *Chem. Rev.* **2007**, *107*, 2891.

3 A. Fujishima, K. Honda, *Nature* **1972**, *238*, 37.

4 D. A. Tryk, A. Fujishima, K. Honda, *Electrochim. Acta* **2000**, *45*, 2363.

5 U. Diebold, *Surf. Sci. Rep.* **2003**, *48*, 53.

6 R. H. West, G. J. O. Beran, W. H. Green, M. Kraft, *J. Phys. Chem. A* **2007**, *111*, 3560.

7 S. E. Pratsinis, P. T. Spicer, *Chem. Eng. Sci.* **1998**, *53*, 1861.

8 J. K. Ani, S. Savithri, G. D. Surender, *Aerosol Air Qual. Res.* **2005**, *5*, 1.

9 A. K. John, G. D. Surender, *J. Mater. Sci.* **2005**, *40*, 2999.

10 A. D. Becke, *J. Chem. Phys.* **1993**, *98*, 5648.

11 C. Lee, W. Yang, R. G. Parr, *Phys. Rev. B* **1988**, *37*, 785.

12 T. Wagener, G. Frenking, *Inorg. Chem.* **1998**, *37*, 1805.

13 A. J. Cohen, P. Mori-Sánchez, W. Yang, *Science* **2008**, *321*, 792.

14 a) A. Savin, in *Recent Developments and Applications of Modern Density Functional Theory*, ed. by J. M. Seminario, Elsevier, Amsterdam, **1996**, p. 327. b) S. F. Sousa, P. A. Fernandes, M. J. Ramos, *J. Phys. Chem. A* **2007**, *111*, 10439.

15 a) C. H. Suresh, N. Koga, *Organometallics* **2001**, *20*, 4333. b) C. H. Suresh, N. Koga, *Organometallics* **2006**, *25*, 1924. c) J. Mathew, N. Koga, C. H. Suresh, *Organometallics* **2008**, *27*, 4666. d) H. Nakazawa, T. Kawasaki, K. Miyoshi, C. H. Suresh, N. Koga, *Organometallics* **2004**, *23*, 117; S. Iwamatsu, P. S. Vijayalakshmi, M. Hamajima, C. H. Suresh, N. Koga, T. Suzuki, S. Murata, *Org. Lett.* **2002**, *4*, 1217.

16 a) C. Adamo, V. Barone, *J. Chem. Phys.* **1998**, *108*, 664. b) Y. Zhao, D. G. Truhlar, *Acc. Chem. Res.* **2008**, *41*, 157.

17 J. P. Perdew, J. A. Chevary, S. H. Vosko, K. A. Jackson, M. R. Pederson, D. J. Singh, C. Fiolhais, *Phys. Rev. B* **1992**, *46*, 6671.

18 J. P. Perdew, J. A. Chevary, S. H. Vosko, K. A. Jackson, M. R. Pederson, D. J. Singh, C. Fiolhais, *Phys. Rev. B* **1993**, *48*, 4978.

19 C. Møller, M. S. Plesset, *Phys. Rev.* **1934**, *46*, 618.

20 J. S. Binkley, J. A. Pople, *Int. J. Quantum Chem.* **1975**, *9*, 229.

21 M. J. Frisch, G. W. Trucks, H. B. Schlegel, G. E. Scuseria, M. A. Robb, J. R. Cheeseman, J. A. Montgomery, Jr., T. Vreven, K. N. Kudin, J. C. Burant, J. M. Millam, S. S. Iyengar, J. Tomasi, V. Barone, B. Mennucci, M. Cossi, G. Scalmani, N. Rega, G. A. Petersson, H. Nakatsuji, M. Hada, M. Ehara, K. Toyota, R.

Fukuda, J. Hasegawa, M. Ishida, T. Nakajima, Y. Honda, O. Kitao, H. Nakai, M. Klene, X. Li, J. E. Knox, H. P. Hratchian, J. B. Cross, V. Bakken, C. Adamo, J. Jaramillo, R. Gomperts, R. E. Stratmann, O. Yazyev, A. J. Austin, R. Cammi, C. Pomelli, J. W. Ochterski, P. Y. Ayala, K. Morokuma, G. A. Voth, P. Salvador, J. J. Dannenberg, V. G. Zakrzewski, S. Dapprich, A. D. Daniels, M. C. Strain, O. Farkas, D. K. Malick, A. D. Rabuck, K. Raghavachari, J. B. Foresman, J. V. Ortiz, Q. Cui, A. G. Baboul, S. Clifford, J. Cioslowski, B. B. Stefanov, G. Liu, A. Liashenko, P. Piskorz, I. Komaromi, R. L. Martin, D. J. Fox, T. Keith, M. A. Al-Laham, C. Y. Peng, A. Nanayakkara, M. Challacombe, P. M. W. Gill, B. Johnson, W. Chen, M. W. Wong, C. Gonzalez, J. A. Pople, *Gaussian 03, Revision C.02*, Gaussian, Inc., Wallingford CT, **2004**.

22 a) C. Gonzalez, H. B. Schlegel, *J. Chem. Phys.* **1989**, *90*, 2154. b) C. Gonzalez, H. B. Schlegel, *J. Phys. Chem.* **1990**, *94*, 5523.

23 Y. Morino, H. Uehara, *J. Chem. Phys.* **1966**, *45*, 4543.

24 X. Wang, L. Andrews, *J. Phys. Chem. A* **2005**, *109*, 10689.

25 G. W. A. Fowles, F. H. Pollard, *J. Chem. Soc.* **1953**, *527*, 2588.

26 V. Jonas, G. Frenking, M. T. Reetz, *J. Comput. Chem.* **1992**, *13*, 919.

27 M. Siodmiak, G. Frenking, A. Korkin, *J. Mol. Model.* **2000**, *6*, 413.

28 S. K. Ignatov, P. G. Sennikov, A. G. Razuvaev, L. A. Chuprov, O. Schrems, B. S. Ault, *J. Phys. Chem. A* **2003**, *107*, 8705.

29 M. Ritala, M. Leskelä, L.-S. Johansson, L. Niinistö, *Thin Solid Films* **1993**, *228*, 32.

30 H. Kumagai, M. Matsumoto, K. Toyoda, M. Obara, M. Suzuki, *Thin Solid Films* **1995**, *263*, 47.

31 J. Aarik, A. Aidla, V. Sammelselg, H. Siimon, T. Uustare, *J. Cryst. Growth* **1996**, *169*, 496.

32 J. Aarik, A. Aidla, H. Mändar, V. Sammelselg, *J. Cryst. Growth* **2000**, *220*, 531.